

Manipulating the Relaxation Time of Boundary-Dissipative Systems through Bond Dissipation

Yi Peng,^{1,*} Chao Yang,^{2,1,3,*} and Yucheng Wang^{2,1,3,†}

¹International Quantum Academy, Shenzhen 518048, China

²Shenzhen Institute for Quantum Science and Engineering,

Southern University of Science and Technology, Shenzhen 518055, China

³Guangdong Provincial Key Laboratory of Quantum Science and Engineering,
Southern University of Science and Technology, Shenzhen 518055, China

Relaxation time plays a crucial role in describing the relaxation processes of quantum systems. We study the effect of a type of bond dissipation on the relaxation time of boundary dissipative systems and find that it can change the scaling of the relaxation time $T_c \sim L^z$ from $z = 3$ to a value significantly less than 3. We further reveal that the reason such bond dissipation can significantly reduce the relaxation time is that it can selectively target specific states. For Anderson localized systems, the scaling behavior of the relaxation time changes from an exponential form to a power-law form as the system size varies. This is because the bond dissipation we consider can not only select specific states but also disrupt the localization properties. Our work reveals that in open systems, one type of dissipation can be used to regulate the effects produced by another type of dissipation.

Introduction.— Relaxation processes of quantum systems interacting with their environments are among the most foundational nonequilibrium phenomena. A piece of material in contact with baths at its two boundaries can reach a nonequilibrium steady state, corresponding to the simplest scenario of nonequilibrium systems [1]. In recent years, with the development of experimental techniques providing us with various highly controllable platforms to study the dynamics of open quantum systems [2–12], significant advances have also been made in the study of quantum systems coupled to different baths at their edges [1, 13–24]. A pivotal inquiry here pertains to determining the timescale for a boundary-dissipative system to attain a steady state. The Liouvillian gap remains an important quantity for characterizing the relaxation time. Except in some special cases [24–30], the relaxation timescale can usually be estimated by the inverse of the Liouvillian gap [24, 30–33]. Previous results have shown that for various boundary-dissipated systems, the Liouvillian gap Δ_g scales with the system length L as $\Delta_g \sim L^{-3}$ for integrable systems [14, 24, 34–37] and $\Delta_g \sim e^{-L/l}$ for Anderson localization (AL) systems [31, 38], with l being the localization length. Consequently, the corresponding scaling of the relaxation time is $T_c \sim L^3$ and $T_c \sim e^{L/l}$, respectively.

In this letter, we investigate how to manipulate the relaxation time of a quantum system with boundary dissipation. This issue holds significant relevance in applications, as regulating the relaxation time is essential for transport properties, quantum control, and information processing. Apart from the particle number decay at the boundaries, we introduce a type of bond dissipation that can be realized experimentally. This type of dissipation conserves the particle number. However, we find that it can change the scaling of the relaxation time $T_c \sim L^z$ from $z = 3$ to a value of z significantly less than 3. In other words, it can significantly reduce the relaxation

time, especially when the system size is large, allowing the system to reach equilibrium more quickly. When this type of dissipation is applied to a localized system with boundary dissipation, the scaling behavior of the relaxation time changes from an exponential form to a power-law form as the system size varies. We further elucidate the mechanism by which this bond dissipation reduces the relaxation time. Since this type of dissipation can be experimentally realized, it can be used to regulate the relaxation time of boundary-dissipative systems.

Model and results.— We consider the simplest one-dimensional model with only nearest-neighbor hopping, whose Hamiltonian is given by

$$H_0 = -J \sum_{m=1}^{L-1} \left(c_{m+1}^\dagger c_m + c_m^\dagger c_{m+1} \right), \quad (1)$$

where c_m (c_m^\dagger) is the annihilation (creation) operator for a particle at site m , and J is the hopping amplitude between neighboring sites, which is set to 1 as the unit energy. We consider a boundary-dissipative system where the particle loss operator acts only on the first and last sites of the lattice. This can be described by a purely imaginary on-site potential,

$$V_{\text{nh}} = -i\gamma \left(c_1^\dagger c_1 + c_L^\dagger c_L \right). \quad (2)$$

We then introduce bond dissipation acting on a pair of sites m and $m + \ell$, described by [39–47]

$$D_m = \left(c_m^\dagger + a c_{m+\ell}^\dagger \right) (c_m - a c_{m+\ell}), \quad (3)$$

where $a = 1$ or -1 , $\ell = 1$ or 2 , and $m = 1, \dots, L - \ell$. This type of dissipation can be realized through cold atoms in optical superlattices [39–43] or through arrays of superconducting microwave resonators [44, 45]. This operator obviously does not change the number of particles in the

system, but it does alter the relative phase between this pair of sites separated by a distance ℓ . They are synchronized from an out-of-phase mode to an in-phase mode (or vice versa) by this operator when a is set to 1 (or -1). This property is important for driving a system to a specific steady state and thereby reducing the relaxation time of the boundary-dissipative system, as will become evident below.

The dissipative dynamics of density matrix $\rho(t)$ is described by the Lindblad master equation [48, 49]

$$\frac{d\rho(t)}{dt} = \mathcal{L}[\rho(t)] = -i [H_{\text{tot}}\rho(t) - \rho(t)H_{\text{tot}}^\dagger] + \mathcal{D}[\rho(t)], \quad (4)$$

where the Hamiltonian $H_{\text{tot}} = H_0 + V_{\text{nh}}$ is non-Hermitian, \mathcal{L} is called the Lindbladian superoperator and \mathcal{D} is the dissipation superoperator

$$\mathcal{D}[\rho(t)] = \Gamma \sum_m \left[D_m \rho D_m^\dagger - \frac{1}{2} \{ D_m^\dagger D_m, \rho \} \right]. \quad (5)$$

which contains a set of jump operators D_m as shown in Eq. (3), all with the same strength Γ . We set $\Gamma = 1$

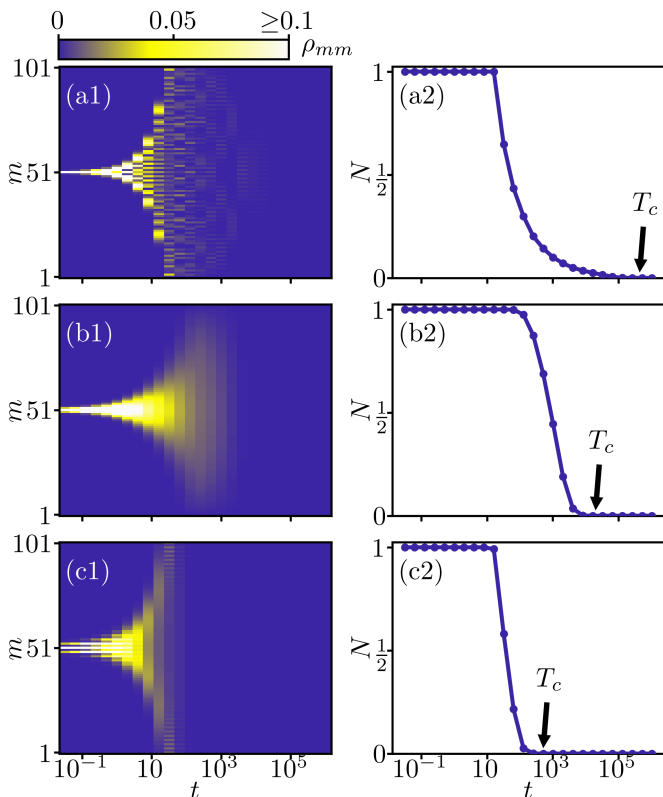


Figure 1: The occupation probability ρ_{mm} of each lattice site [(a1), (b1), (c1)] and the total number of particles N [(a2), (b2), (c2)] change over time for (a1) and (a2) $\Gamma = 0$; (b1) and (b2) $\Gamma = 1$, $\ell = 1$ and $a = 1$; and (c1) and (c2) $\Gamma = 1$, $\ell = 2$ and $a = -1$. The initial state is set at the center of the system, with a fixed size of $L = 101$. T_c corresponds to the time when N decreases to 10^{-7} .

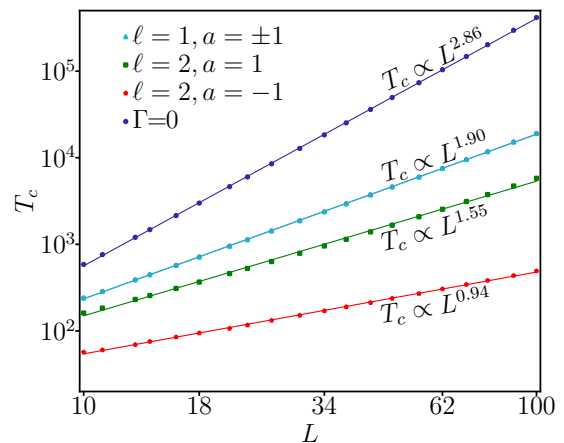


Figure 2: The relaxation time T_c varies with size L . Numerical fitting results: $T_c \sim L^{2.86}$ if $\Gamma = 0$; $T_c \sim L^{1.9}$ if $\ell = 1$ and $a = \pm 1$; $T_c \sim L^{0.94}$ if $\ell = 2$ and $a = -1$; and $T_c \sim L^{1.55}$ if $\ell = 2$ and $a = 1$.

and boundary dissipation strength $\gamma = 0.5$ without loss of generality. Since \mathcal{L} is time-independent, one can express $\rho(t) = e^{\mathcal{L}t}\rho(0)$. In our numerical simulation, we adopt the 4th-order Runge-Kutta method to integrate the master equation and thereby calculate the time evolution superoperator $e^{\mathcal{L}t}$.

To visually observe the impact of bond dissipation D_m on the relaxation time of the boundary-dissipative system, we first examine the change in particle occupancy over time. A particle is initially placed at the center of the system, i.e., $\rho(0) = |\frac{L+1}{2}\rangle\langle\frac{L+1}{2}|$ (let L be odd). For any time t , we can record the occupation probability $\rho_{mm}(t) = \langle m|\rho(t)|m\rangle$ of every site m , as shown in Figs. 1(a1, b1, c1), and calculate the total number of particles $N(t) = \sum_m \rho_{mm}(t)$, as shown in Figs. 1(a2, b2, c2). The particle will eventually escape the lattice, and all ρ_{mm} as well as N will approach zero as time passes, regardless of whether there is bond dissipation [Figs. 1(b1, b2, c1, c2)] or not [Figs. 1(a1, a2)]. However, bond dissipation does accelerate the particle loss process. To quantitatively characterize this acceleration effect, we use a cutoff of total particle number $N = 10^{-7}$, that is, we evaluate the system's relaxation time T_c when $N = 10^{-7}$. From Figs. 1(a2), (b2), and (c2), it can be seen that, compared with the case without bond dissipation, when the dissipation with $\ell = 1$ and $a = 1$ ($\ell = 2$ and $a = -1$) is added, the relaxation time T_c is reduced to approximately 1/20 (1/800) of its original value.

Next, we study the relationship between the relaxation time T_c and the system size. Fig. 2 shows that regardless of the presence of bond dissipation, the relationship between the relaxation time and the system size for the boundary dissipative system can be expressed as $T_c \sim L^z$. When there is no bond dissipation, z is approximately 2.86, which is consistent with the result $z \approx 3$ within the error range. However, when bond dissipation is present,

z is significantly less than 2.86, and the magnitude of z also clearly depends on the specific form of bond dissipation, i.e., on ℓ and a . We observe that when $\ell = 1$, the value of z is approximately the same for $a = 1$ and $a = -1$, around 1.9. When $\ell = 2$ and $a = -1$, z is minimized, indicating that in this case, the reduction effect of bond dissipation on the relaxation time is most significant, which is consistent with the results in Fig. 1.

We now analyze the reason why the particle number conserving bond dissipation D_m can significantly reduce the relaxation time of the boundary-dissipative system. The relaxation time T_c here is inversely proportional to the Liouvillian spectral gap Δ_g , which is defined as the minimum absolute value of the real part of the nonzero eigenvalues of the Liouvillian superoperator. Without bond dissipation, i.e., when $\Gamma = 0$, Δ_g is twice the smallest modulus of the imaginary part of the nonzero eigenvalues of the total Hamiltonian H_{tot} . We can sort the eigenlevels of H_{tot} in ascending order of their real parts, which are mainly determined by the eigenlevels of H_0 since V_{nh} can be considered a perturbative term when L is sufficiently large. The index of the energy mode is denoted as n_E , and then we introduce a size-independent quantity $\epsilon = (n_E - 1)/(L - 1)$. Clearly, the smallest, middle and largest real parts of the eigenvalues of H_{tot} correspond to $\epsilon = 0$, $\epsilon = 0.5$ and $\epsilon = 1$, respectively.

We examine the absolute value of the imaginary part of each eigenvalue, denoted as Δ , as the system size changes. Fig. 3(a) shows $\Delta \propto 1/L^3$ when the corresponding real part is the smallest (i.e., $\epsilon = 0$) and $\Delta \propto 1/L$ when the corresponding real part is in the middle of the spectrum (i.e., $\epsilon = 1/2$). It is easy to verify numerically that the relationship between the absolute value of the imaginary part Δ of all eigenvalues and the system size satisfies $\Delta \propto 1/L^\alpha$. We show the variation of α with ϵ in Fig. 3(b). It can be seen that α has its highest value of 3 at the smallest and largest real parts ($\epsilon = 0$ and $\epsilon = 1$), and its lowest value of 1 for most ϵ within $(0, 1)$, except for a few levels close to the bottom (top) of the eigenlevels of H_{tot} . This creates a cup shape with a wide, flat bottom, as shown in Fig. 3(b). It can be conjectured that the previously discovered $T_c \sim L^3$ scaling behavior mainly originates from the states at $\epsilon = 0$ and $\epsilon = 1$. This is also consistent with Fig. 3(a), where Δ at $\epsilon = 0$ is significantly smaller than the value at $\epsilon = 0.5$, and the relaxation time is determined by the smallest Δ . To further confirm this point, we introduce

$$P(t) = (\langle \psi_1 | \rho(t) | \psi_1 \rangle + \langle \psi_L | \rho(t) | \psi_L \rangle) / \text{Tr} \rho(t). \quad (6)$$

It describes the ratio of the sum of the particle numbers in the state ψ_1 at $\epsilon = 0$ and the state ψ_L at $\epsilon = 1$ to the total particle number at any time t [50]. As seen in Fig. 3(c), when there is no bond dissipation (i.e., $\Gamma = 0$), after a certain period of time, all states except ψ_1 and ψ_L dissipate, and P is approximately equal to 1.

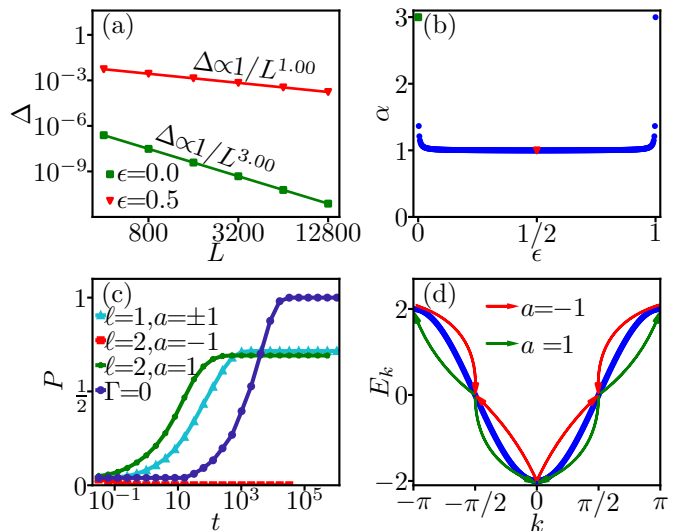


Figure 3: (a) The absolute value of the imaginary part Δ of the eigenvalues with the smallest real part ($\epsilon = 0$) and the middle real part ($\epsilon = 0.5$) of H_{tot} varies with the system size L . (b) Inverse scaling coefficient α of $\Delta \propto 1/L^\alpha$ for all ϵ . (c) Without bond dissipation and with bond dissipation under different parameters, the change of occupation rate P over time t . (d) A schematic diagram of the physical effects generated by bond dissipation with $\ell = 2$.

This proves that the relaxation time of this boundary-dissipative system is determined by the states at $\epsilon = 0$ and $\epsilon = 1$, hence $T_c \sim L^3$. When bond dissipation with $\ell = 2$ and $a = -1$ is added, P quickly becomes 0. Therefore, the states at $\epsilon = 0$ and $\epsilon = 1$ do not determine its boundary dissipation, which explains its scaling behavior $T_c \sim L^z$ with $z \approx 1$. When the bond dissipation with other parameters is added, P eventually stabilizes at a value between 0 and 1. Therefore, the relaxation time is influenced by the states at $\epsilon = 0$ and $\epsilon = 1$, but not solely determined by them. Consequently, the scaling behavior of the relaxation time with size is given by $T_c \sim L^z$, where z lies between 1 and 3.

The behavior of P over time shown in Fig. 3(c) can be understood through the influence of bond dissipation on the eigenstates of H_0 . Its eigenvalue is given by $E = -2J \cos(k)$ and wave function is e^{ikm} , with $k = 2\pi n/L$ ($n \in (-L/2, L/2]$), and the phase difference between the next-nearest neighbor (NNN) lattice sites is $\Delta\phi = 2k$. For the states at the bottom ($k = 0$) and top ($k = \pi$) of the energy band, the NNN sites are in phase. For the states in the middle of the energy band ($k = \pi/2$), the NNN sites are out of phase. Therefore, when $a = -1$, this bond dissipation annihilates the in-phase states and produces out-of-phase states, as shown by the red line in Fig. 3(d). This results in only the states near the middle of the spectrum participating in the boundary dissipation behavior, as indicated by $P = 0$ in Fig. 3(c). When $a = 1$, this bond dissipation annihilates the out-of-phase states

and produces in-phase states, as shown by the green line in Fig. 3(d). Therefore, P is a non-zero value, but it is also never equal to 1 (see Supplementary Material [51]). The particles in the states with $\alpha = 1$ are more easily dissipated, but this bond dissipation forces the proportions of each state to remain constant. This leads to particles from the $\alpha = 3$ states transitioning into the $\alpha = 1$ states to maintain the constant proportions, as shown in Fig. 3(c), which in turn results in the shortening of the relaxation time of boundary-dissipative systems. Similarly, the variation of P over time for $l = 1$ can be understood.

In the presence of Anderson localization.— Finally, we consider the impact of bond dissipation shown in Eq. (3) on the relaxation time of boundary-dissipative systems in the presence of AL. AL can be induced by either a random on-site potential

$$V_{\text{rand}} = \sum_{m=1}^L V_m c_m^\dagger c_m, \quad (7)$$

where V_m is uniformly distributed in $[-W/2, W/2]$ with W being the disorder strength of the system, or a quasiperiodic potential,

$$V_{\text{qp}} = V \sum_{m=1}^L \cos(2\pi\beta m + \theta) c_m^\dagger c_m, \quad (8)$$

where β is an irrational number, and V and θ are the strength and initial phase of the quasiperiodic potential, respectively. $H = H_0 + V_{\text{qp}}$ is the Aubry-André model [52], which exhibits an Anderson transition at $V/J = 2$. When $V/J > 2$ (or $V/J < 2$), all eigenstates are localized (or extended). When the added potential is random disorder, i.e., V_{qp} is replaced with V_{rand} , any weak disorder strength W can cause the system to become localized. In the absence of bond dissipation, the relaxation time of boundary dissipation undergoes an exponential scaling relation with the change in system size $T_c \propto e^{\eta L}$ in the AL phase [31, 38], as shown in Fig. 4(a). This is because an electron localized within the bulk of the lattice has an exponentially small chance, relative to L , of reaching the particle loss channel at the lattice boundaries. When bond dissipation D_m is introduced, we observe that the scaling behavior of the relaxation time changes to a power-law form as the system size varies [Fig. 4(a)]. This cannot be explained by the previous property of D_m selectively targeting specific states, because now all states are localized in the absence of D_m . This indicates that this bond dissipation may disrupt the localized nature of the states. To verify this, we set the strength of boundary dissipation $\gamma = 0$ and study the impact of bond dissipation on the wave packet dynamics of this localized system. A common quantity used to describe the dynamics of wave packet evolution is the mean

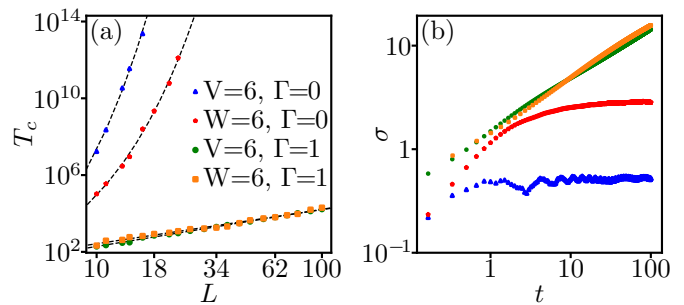


Figure 4: In the AL phase, (a) the change of relaxation time with system size both with and without bond dissipation, and (b) the evolution of σ over time. (a) When $\Gamma = 0$, to smooth the data, we averaged over 1000 samples for both disordered and quasi-periodic systems. For the quasi-periodic system, each sample corresponds to an initial phase θ . When $\Gamma \neq 0$, taking multiple samples has little effect on the results. (b) $\kappa = 0.478$ for $V = 6, \Gamma = 1$ and $\kappa = 0.518$ for $W = 6, \Gamma = 1$. Here we take $\beta = (\sqrt{5} - 1)/2$ and the bond dissipation with $\ell = 1$ and $a = 1$, and the effect on the results is similar when β, ℓ and a take other values.

square displacement [53–56]

$$\sigma(t) = \sqrt{\sum_m [m - (L + 1)/2]^2 \rho_{mm}(t)}. \quad (9)$$

which measures the width of the wave packet initially located at the center of the system, with L taken as an odd number. After a period of time, the change of σ over time can be expressed as $\sigma \sim t^\kappa$, where the dynamical index κ corresponds to different types of diffusion: $\kappa = 0$ for localized, $\kappa < 1/2$ for subdiffusive, $\kappa \approx 1/2$ for normal diffusive, $\kappa > 1/2$ for superdiffusive, and $\kappa = 1$ for ballistic diffusion. From Fig. 4(b), we can see that when there is no bond dissipation ($\Gamma = 0$), the system is localized. With the addition of bond dissipation, the wave packet evolution approaches normal diffusion. This explains why the scaling relation of the relaxation time with system size in the boundary-dissipative system changes from an exponential form to a power-law form.

Conclusion and Discussion.— We have investigated the impact of bond dissipation shown in Eq. (3) on the relaxation time of boundary-dissipative systems, and found that bond dissipation can significantly reduce the relaxation time. The scaling of the relaxation time $T_c \sim L^z$ changes from $z = 3$ to a value significantly less than 3. This is because bond dissipation can selectively target specific states, thereby eliminating or reducing the influence of the states with the longest relaxation times. For Anderson localized systems, bond dissipation can change the scaling behavior of the relaxation time from an exponential form to a power-law form as the system size varies. This is because bond dissipation disrupts the localization properties of the system, making it more akin to normal diffusive behavior. Our results highlight

the significant role of bond dissipation in manipulating the relaxation processes of quantum systems.

For simplicity, we mainly discussed the case where both boundaries are particle loss channels. If one side is gain and the other is loss, the results we present regarding the impact of bond dissipation on the relaxation time still apply. Additionally, we primarily discussed the case where the boundary dissipation strength $\gamma < 1$. In the Supplementary Material [51], we present the results for $\gamma = 1$ and $\gamma > 1$. We can observe that states at the center of the energy spectrum seem to exhibit a phase transition-like behavior when $\gamma = 1$. This change can be measured through the bond dissipation with $\ell = 2$ and $a = -1$. Our results also introduce some interesting questions worthy of further investigation. For instance, how does bond dissipation affect the relaxation time of boundary-dissipative systems in the presence of interactions? How does this impact change in the presence of many-body localization? Can this bond dissipation also regulate the relaxation time in systems with other types of dissipation?

This work is supported by National Key R&D Program of China under Grant No.2022YFA1405800, the National Natural Science Foundation of China (Grant No.12104205), the Key-Area Research and Development Program of Guangdong Province (Grant No. 2018B030326001), Guangdong Provincial Key Laboratory (Grant No.2019B121203002).

* These authors contribute equally to this work.

† Corresponding author: wangyc3@sustech.edu.cn

- [1] G. T. Landi, D. Poletti, and G. Schaller, Nonequilibrium boundary-driven quantum systems: Models, methods, and properties, *Rev. Mod. Phys.* **94**, 045006 (2022).
- [2] I. Bloch, Quantum coherence and entanglement with ultra cold atoms in optical lattices, *Nature (London)* **453**, 1016 (2008).
- [3] S. Diehl, A. Micheli, A. Kantian, B. Kraus, H.P. Büchler, and P. Zoller, Quantum states and phases in driven open quantum systems with cold atoms, *Nat. Phys.* **4**, 878 (2008).
- [4] N. Syassen, D. M. Bauer, M. Lettner, T. Volz, D. Dietze, J. J. García-Ripoll, J. I. Cirac, G. Rempe, and S. Dürr, Strong Dissipation Inhibits Losses and Induces Correlations in Cold Molecular Gases, *Science*, **320**, 5881, (2008).
- [5] H. Weimer, R. Löw, T. Pfau, and H.P. Büchler, Quantum critical behavior in strongly interacting Rydberg gases, *Phys. Rev. Lett.* **101**, 250601 (2008).
- [6] T. E. Lee, H. Häffner, and M.C. Cross, Antiferromagnetic phase transition in a nonequilibrium lattice of Rydberg atoms, *Phys. Rev. A* **84**, 031402(R) (2011).
- [7] A. Tomadin, S. Diehl, and P. Zoller, Nonequilibrium phase diagram of a driven and dissipative many-body system, *Phys. Rev. A* **83**, 013611 (2011).
- [8] M. Ludwig and F. Marquardt, Quantum many-body dynamics in optomechanical arrays, *Phys. Rev. Lett.* **111**, 073603 (2013).
- [9] S. Viciani, M. Lima, M. Bellini, and F. Caruso, Observation of noise-assisted transport in an all-optical cavity-based network, *Phys. Rev. Lett.* **115**, 083601 (2015).
- [10] C. Maier, T. Brydges, P. Jurcevic, N. Trautmann, C. Hempel, B. P. Lanyon, P. Hauke, R. Blatt, and C. F. Roos, Environment assisted quantum transport in a 10-Qubit network, *Phys. Rev. Lett.* **122**, 050501 (2019).
- [11] Y. Sun, T. Shi, Z. Liu, Z. Zhang, L. Xiao, S. Jia, and Y. Hu, Fractional Quantum Zeno Effect Emerging from Non-Hermitian Physics, *Phys. Rev. X* **13**, 031009 (2023).
- [12] L. Li, T. Liu, X.-Y. Guo, H. Zhang, S. Zhao, Z. Xiang, X. Song, Y.-X. Zhang, K. Xu, H. Fan, and D. Zheng, Observation of multiple steady states with engineered dissipation, arXiv:2308.13235.
- [13] B. Buča and T. Prosen, Exactly Solvable Counting Statistics in Open Weakly Coupled Interacting Spin Systems, *Phys. Rev. Lett.* **112**, 067201, (2014).
- [14] T. Prosen and I. Pizorn, Quantum phase transition in a far from equilibrium steady state of an XY spin chain, *Phys. Rev. Lett.* **101**, 105701 (2008).
- [15] D. Karevski, V. Popkov, and G. M. Schütz, Exact Matrix Product Solution for the Boundary-Driven Lindblad XXZ Chain, *Phys. Rev. Lett.* **110**, 047201 (2013).
- [16] V. Popkov, T. Prosen, and L. Zadnik, Exact Nonequilibrium Steady State of Open XXZ/XYZ Spin-1/2 Chain with Dirichlet Boundary Conditions, *Phys. Rev. Lett.* **124**, 160403 (2020).
- [17] C. Guo and D. Poletti, Analytical solutions for a boundary-driven XY chain, *Phys. Rev. A* **98**, 052126 (2018).
- [18] A. M. Lacerda, J. Goold, and G. T. Landi, Dephasing enhanced transport in boundary-driven quasiperiodic chains, *Phys. Rev. B* **104**, 174203 (2021).
- [19] F. Tarantelli and E. Vicari, Quantum critical systems with dissipative boundaries, *Phys. Rev. B* **104**, 075140 (2021).
- [20] F. Carollo, J. P. Garrahan, I. Lesanovsky, and C. Pérez-Espigares, Fluctuating hydrodynamics, current fluctuations, and hyperuniformity in boundary-driven open quantum chains, *Phys. Rev. E* **96**, 052118 (2017).
- [21] M. Saha, B. P. Venkatesh, and B. K. Agarwalla, Quantum transport in quasiperiodic lattice systems in the presence of Büttiker probes, *Phys. Rev. B* **105**, 224204 (2022).
- [22] V. Balachandran, S. R. Clark, J. Goold, and D. Poletti, Energy Current Rectification and Mobility Edges, *Phys. Rev. Lett.* **123**, 020603 (2019).
- [23] A. Lingenfelter, M. Yao, A. Pocklington, Y.-X. Wang, A. Irfan, W. Pfaff, and A. A. Clerk, Exact Results for a Boundary-Driven Double Spin Chain and Resource-Efficient Remote Entanglement Stabilization, *Phys. Rev. X* **14**, 021028 (2024).
- [24] M. Žnidarič, Relaxation times of dissipative many-body quantum systems, *Phys. Rev. E* **92**, 042143 (2015).
- [25] T. Mori, Metastability associated with many-body explosion of eigenmode expansion coefficients, *Phys. Rev. Research* **3**, 043137 (2021).
- [26] J. Bensa and M. Žnidarič, Two-step phantom relaxation of out-of-time-ordered correlations in random circuits, *Phys. Rev. Research* **4**, 013228 (2022).
- [27] T. Mori and T. Shirai, Resolving a Discrepancy between Liouvillian Gap and Relaxation Time in Boundary-

- Dissipated Quantum Many-Body Systems, Phys. Rev. Lett. **125**, 230604 (2020).
- [28] G. Lee, A. McDonald, and A. Clerk, Anomalous large relaxation times in dissipative lattice models beyond the non-Hermitian skin effect, Phys. Rev. B **108**, 064311 (2023).
- [29] Z. Wang, Y. Lu, Y. Peng, R. Qi, Y. Wang, and J. Jie, Accelerating Relaxation Dynamics in Open Quantum System with Liouvillian Skin Effect, Phys. Rev. B **108**, 054313 (2023)
- [30] T. Haga, M. Nakagawa, R. Hamazaki, and M. Ueda, Liouvillian Skin Effect: Slowing Down of Relaxation Processes without Gap Closing, Phys. Rev. Lett. **127**, 070402 (2021).
- [31] T. Prosen, Third quantization: a general method to solve master equations for quadratic open Fermi systems, New J. Phys. **10**, 043026 (2008).
- [32] Z. Cai and T. Barthel, Algebraic Versus Exponential Decoherence in Dissipative Many-Particle Systems, Phys. Rev. Lett. **111**, 150403 (2013).
- [33] L. Bonnes, D. Charrier, and A. M. Läuchli, Dynamical and steady-state properties of a Bose-Hubbard chain with bond dissipation: A study based on matrix product operators, Phys. Rev. A **90**, 033612 (2014).
- [34] K. Yamanaka and T. Sasamoto, Exact solution for the Lindbladian dynamics for the open XX spin chain with boundary dissipation, SciPost Phys. **14**, 112 (2023).
- [35] Z.-Y. Zheng, X. Wang, and S. Chen, Exact solution of the boundary-dissipated transverse field Ising model: Structure of the Liouvillian spectrum and dynamical duality, Phys. Rev. B **108**, 024404 (2023).
- [36] F. Tarantelli and E. Vicari, Out-of-equilibrium quantum dynamics of fermionic gases in the presence of localized particle loss, Phys. Rev. A **105**, 042214 (2022); F. Tarantelli and E. Vicari, Quantum critical systems with dissipative boundaries, Phys. Rev. B **104**, 075140 (2021).
- [37] S.-Y. Zhang, M. Gong, G.-C. Guo, and Z.-W. Zhou, Anomalous relaxation and multiple timescales in the quantum XY model with boundary dissipation, Phys. Rev. B **101**, 155150 (2020).
- [38] B. Zhou, X. Wang and S. Chen, Exponential size scaling of the Liouvillian gap in boundary-dissipated systems with Anderson localization, Phys. Rev. B **106**, 064203 (2022).
- [39] S. Diehl, A. Micheli, A. Kantian, B. Kraus, H. P. Büchler, and P. Zoller, Quantum states and phases in driven open quantum systems with cold atoms, Nat. Phys. **4**, 878 (2008).
- [40] B. Kraus, H. P. Büchler, S. Diehl, A. Kantian, A. Micheli, and P. Zoller, Preparation of entangled states by quantum Markov processes, Phys. Rev. A **78**, 042307 (2008).
- [41] S. Diehl, A. Tomadin, A. Micheli, R. Fazio, and P. Zoller, Dynamical Phase Transitions and Instabilities in Open Atomic Many-Body Systems, Phys. Rev. Lett. **105**, 015702 (2010); S. Diehl, E. Rico, M. A. Baranov, P. Zoller, Topology by Dissipation in Atomic Quantum Wires, Nat. Phys. **7**, 971 (2011).
- [42] C.-E. Bardyn, M. A. Baranov, C. V. Kraus, E. Rico, A. Imamoglu, P. Zoller, S. Diehl, Topology by dissipation, New J. Phys. **15**, 085001 (2013).
- [43] Y. Liu, Z. Wang, C. Yang, J. Jie, and Y. Wang, Dissipation induced extended-localized transition, Phys. Rev. Lett. **132**, 216301 (2024).
- [44] D. Marcos, A. Tomadin, S. Diehl, and P. Rabl, Photon condensation in circuit quantum electrodynamics by engineered dissipation, New J. Phys. **14**, 055005 (2012).
- [45] I. Yusipov, T. Lapyteva, S. Denisov, and M. Ivanchenko, Localization in Open Quantum Systems, Phys. Rev. Lett. **118**, 070402 (2017).
- [46] O. S. Vershinina, I. I. Yusipov, S. Denisov, M. V. Ivanchenko, T. V. Lapyteva, Control of a single-particle localization in open quantum systems, Europhys. Lett. **119**, 56001 (2017); I. I. Yusipov, T. V. Lapyteva, M. V. Ivanchenko, Quantum jumps on Anderson attractors, Phys. Rev. B **97**, 020301 (2018); I. Vakulchyk, I. Yusipov, M. Ivanchenko, S. Flach, and S. Denisov, Signatures of many-body localization in steady states of open quantum systems, Phys. Rev. B **98**, 020202(R) (2018).
- [47] T. Haga, Oscillating-mode gap: an indicator of phase transition in open quantum many-body systems, arXiv:2405.07132.
- [48] G. Lindblad, On the generators of quantum dynamical semigroups, Commun. Math. Phys. **48**, 119 (1976).
- [49] H.-P. Breuer and F. Petruccione, *The Theory of Open Quantum Systems* (Oxford University Press, Oxford, 2002).
- [50] We provide a simple understanding that α equals 3 at the spectral boundary and 1 at the spectral center. In the free fermionic model Eq. (1) under open boundary conditions, the eigenvalues are $E_j = -2J \cos \frac{j\pi}{L+1}$, and the corresponding eigenvectors are $|\psi_j\rangle = \sqrt{\frac{2}{L+1}} \sum_{m=1}^L \sin \frac{j m \pi}{L+1} |m\rangle$ with $j = 1, 2, \dots, L$ being the index of eigenstate. The boundary density of states are $D_j = |\psi_{j,1}|^2 + |\psi_{j,L}|^2 = \frac{4}{L+1} \sin^2 \frac{j\pi}{L+1}$. Then from the perturbative perspective, we can show $\Delta_j = -2\gamma D_j$ is proportional to the boundary density of states. Hence near the band edge $j \rightarrow 1$ or L , $\sin^2 \frac{j\pi}{L+1} \sim L^{-2}$, so $\Delta \sim L^{-3}$, while inside the band $j \rightarrow \frac{L}{2}$, we have $\Delta \sim L^{-1}$.
- [51] See Supplemental Material for details on (I) Manipulation effect of bond dissipation; (II) Boundary dissipation strength $\gamma \geq 1$.
- [52] S. Aubry and G. André, Analyticity breaking and Anderson localization in incommensurate lattices, Ann. Israel Phys. Soc. **3**, 133 (1980).
- [53] H. Hiramoto and S. Abe, Dynamics of an Electron in Quasiperiodic Systems. II. Harper's Model, J. Phys. Soc. Jpn. **57**, 1365 (1988).
- [54] R. Ketzmerick, K. Kruse, S. Kraut, and T. Geisel, What determines the spreading of a wave packet?, Phys. Rev. Lett. **79**, 1959 (1997).
- [55] G. Roati, C. D'Errico, L. Fallani, M. Fattori, C. Fort, M. Zaccanti, G. Modugno, M. Modugno, and M. Inguscio, Anderson localization of a non-interacting Bose-Einstein condensate, Nature (London) **453**, 895 (2008).
- [56] Y. Wang, L. Zhang, S. Niu, D. Yu, X.-J. Liu, Realization and detection of non-ergodic critical phases in optical Raman lattice, Phys. Rev. Lett. **125**, 073204 (2020).

Supplementary Material: Manipulating the Relaxation Time of Boundary-Dissipative Systems through Bond Dissipation

In the Supplementary Materials, we first examine the regulatory effect of bond dissipation in the eigenbasis of H_0 . Then we discuss the peculiar behavior exhibited by the relationship between the absolute value of the imaginary part at the center of the spectrum and the system size when the boundary dissipation strength $\gamma \geq 1$.

I. Manipulation effect of bond dissipation

In this section, we set the boundary dissipation strength $\gamma = 0$ and examine the regulatory effect of bond dissipation in the eigenbasis of H_0 . We can calculate the eigenstates and their corresponding eigenvalues of the Liouvillian superoperator \mathcal{L} . The steady state ρ^s , defined as $\rho^s = \lim_{t \rightarrow \infty} \rho(t)$, corresponds to the zero eigenvalue, i.e., $\mathcal{L}[\rho^s] = 0$. We express ρ^s in the eigenbasis of H_0 as shown in Fig. S1. The manipulation effects of the bond dissipation with different parameters ℓ and a are obvious here. Every bond dissipation favors specific part(s) of the eigenlevels of H_0 : (a) $\ell = 1$ and $a = 1$, the bottom; (b) $\ell = 1$ and $a = -1$, the top; (c) $\ell = 2$ and $a = 1$, both the top and the bottom; and (d) $\ell = 2$ and $a = -1$, the middle. Combining the discussion in our main text, we can understand why the bond dissipation with $\ell = 2$ and $a = -1$ reduces the relaxation time of boundary dissipation the most. For other ℓ and a , although bond dissipation drives the steady state to occupy the edges of the energy spectrum, it still includes many states. Therefore, in the main text, the sum of the proportions of the lowest and highest states is not equal to 1.

Since the relaxation time of boundary dissipation is much longer than the time for the system to reach a steady state due to bond dissipation, it can be assumed that bond dissipation has already distributed the states before the boundary dissipation process begins. The distribution of states is such that the proportion of each state is the same as the steady-state distribution caused by bond dissipation when $\gamma = 0$. Although boundary dissipation reduces the total number of particles, this proportion remains constant.

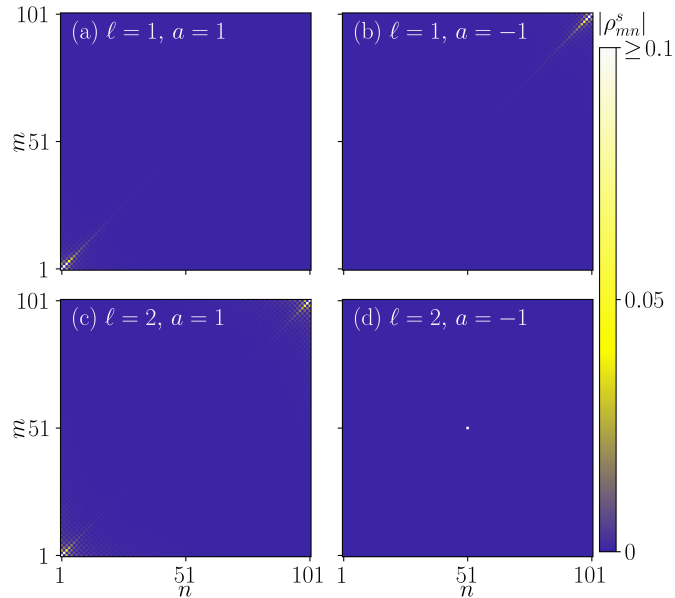


Figure S1: In the eigenbasis of the Hamiltonian H_0 , the absolute values of the density matrix elements ρ_{mn}^s for steady states with (a) $\ell = 1$ and $a = 1$, (b) $\ell = 1$ and $a = -1$, (c) $\ell = 2$ and $a = 1$, and (d) $\ell = 2$ and $a = -1$. Here $L = 101$, $\gamma = 0$, $\Gamma = 1$, m and n are the indices of the eigenstates of H_0 .

II. Boundary dissipation strength $\gamma \geq 1$

In the main text, we have choose the particle-loss strength $\gamma = 0.5$ to avoid the case where $\gamma \geq 1$. When $\gamma = 1$, the dependence of the absolute value of the imaginary part at $\epsilon = 0.5$ on the system size follows $\Delta \sim 1/L^\alpha$, with α being less than 1, approximately 0.87 [see Fig. S2(a1)]. By comparing Fig. S2(a2) with Fig. 3(b) in the main text, it can be seen that only α at $\epsilon = 0.5$ decreases, while the rest remains the same as for $\gamma < 1$. When $\gamma > 1$, the dependence of the absolute value of the imaginary part at $\epsilon = 0.5$ on the system size no longer follows $\Delta \sim 1/L^\alpha$, but instead exhibits large oscillations [see Fig. S2(b1)]. These oscillations occur only at $\epsilon = 0.5$ [see Fig. S2(b2)]. We emphasize that when $\gamma \geq 1$, the change in the absolute value of the imaginary part at $\epsilon = 0.5$ is difficult to detect without bond dissipation because the relaxation time is mainly determined by the eigenvalues near $\epsilon = 0$ and $\epsilon = 1$. Therefore, the change caused by γ does not affect the scaling relationship $T_c \sim L^3$. However, when bond dissipation with $\ell = 2$ and $a = -1$ is introduced, the system's relaxation time is primarily determined by the eigenvalues near $\epsilon = 0.5$. At this point, the changes brought by $\gamma \geq 1$ can be detected.

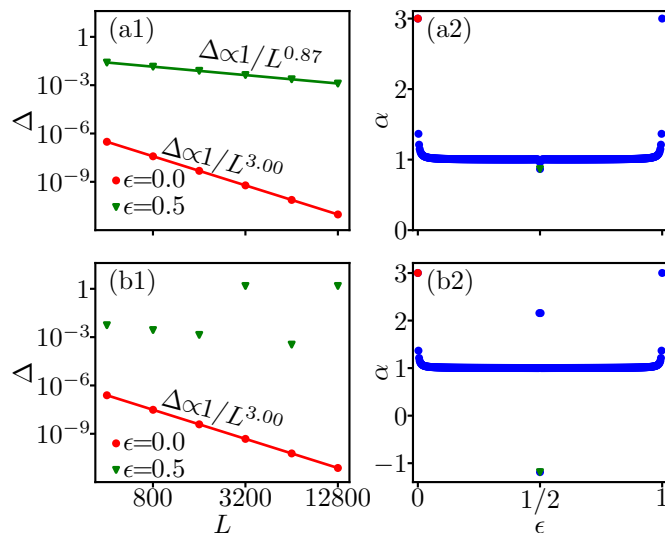


Figure S2: Scaling of the absolute Δ of imaginary part of eigenlevels at $\epsilon = 0$ and $\epsilon = 0.5$ of the total Hamiltonian H_{tot} for (a1) $\gamma = 1$ and (b1) $\gamma = 2$; and inverse scaling coefficient α of $\Delta \propto 1/L^\alpha$ versus ϵ for (a2) $\gamma = 1$ and (b2) $\gamma = 2$.